European Spine Journal (2019) 28:798–806
https://doi.org/10.1007/s00586-018-5847-y

ORIGINAL ARTICLE

Three-dimensionally printed vertebrae with different bone densities for surgical training

Marco Burkhard[1] · **Philipp Fürnstahl**[2] · **Mazda Farshad**[1]

Received: 1 July 2018 / Revised: 21 October 2018 / Accepted: 27 November 2018 / Published online: 3 December 2018

Abstract

Purpose To evaluate whether 3D-printed vertebrae offer realistic haptic simulation of posterior pedicle screw placement and decompression surgery with normal to osteoporotic-like properties.

Methods A parameterizable vertebra model was developed, adjustable in cortical and cancellous bone thicknesses. Based on this model, five different L3 vertebra types (α, β, γ1, γ2, and γ3) were designed and fourfold 3D-printed. Four spine surgeons assessed each vertebra type and a purchasable L3 Sawbones vertebra. Haptic behavior of six common steps in posterior spine surgery was rated from 1 to 10: 1–2: too soft, 3–4: osteoporotic, 5–6: normal, 7–8: hard, and 9–10: too hard. Torques were measured during pedicle screw insertion.

Results In total, 24 vertebrae (six vertebra types times four examiners) were evaluated. Mean surgical assessment scores were: α 3.2 ± 0.9 (osteoporotic), β 1.9 ± 0.7 (too soft), γ1 4.7 ± 0.9 (osteoporotic–normal), γ2 6.3 ± 1.1 (normal), and γ3 7.5 ± 1.1 (hard). All surgeons considered the 3D-printed vertebrae α, γ1, and γ2 as more realistic than Sawbones vertebrae, which were rated with a mean score of 4.1 ± 1.7 (osteoporotic–normal). Mean pedicle screw insertion torques (Ncm) were: α 32 ± 4, β 12 ± 3, γ1 74 ± 4, γ2 129 ± 13, γ3 196 ± 34 and Sawbones 90 ± 11.

Conclusions In this pilot study, 3D-printed vertebrae displayed haptically and biomechanically realistic simulation of posterior spinal procedures and outperformed Sawbones. This approach enables surgical training on bone density-specific vertebrae and provides an outlook toward future preoperative simulation on patient-specific spine replicas.

Graphical abstract These slides can be retrieved under Electronic Supplementary Material.

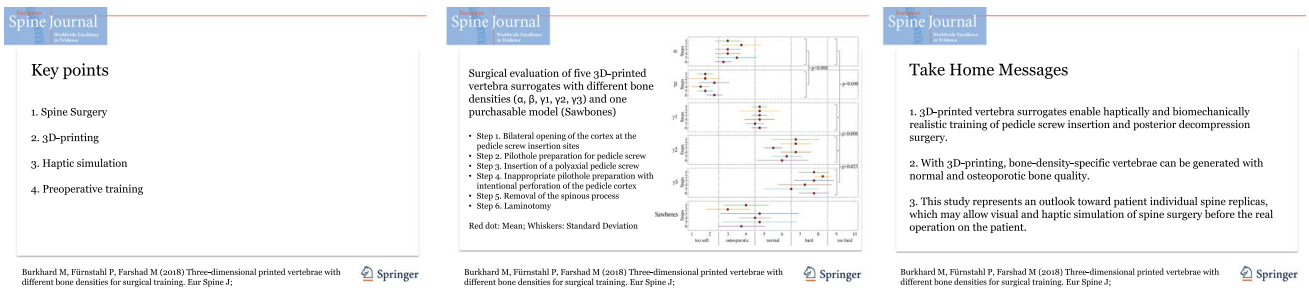

Keywords Spine surgery · 3D printing · Haptic simulation · Preoperative training

Introduction

Spinal fusion surgery with posterior pedicle screws is considered the gold standard in the surgical correction of spinal deformities, fractures, and tumors [1, 2]. Thus, pedicle screw fixation is an essential skill spine surgeons have to master, but high levels of expertise and knowledge about

Electronic supplementary material The online version of this article (https://doi.org/10.1007/s00586-018-5847-y) contains supplementary material, which is available to authorized users.

✉ Marco Burkhard
marco.burkhard@gmail.com

Extended author information available on the last page of the article

the anatomic landmarks are of paramount importance [3]. Screw misplacement may lead to nonunion, irritation of nerve roots, dural lesions, pedicle fractures, and vascular injuries [4, 5].

In traditional surgical education, which has been successful for generations, trainees perform surgery on real patients under supervision of experienced surgeons. However, with rapidly developing alterations in surgical procedures and the heightened focus on patient safety, the demand for training options in a low-stress environment is increasing. As an adjunct to the hands-on clinical experience, surgical training on cadavers, bone replicas, and computer simulators is continuing to gain in importance [6]. In recent years, three-dimensional (3D) printing has entered the field of modern spine surgery and its education, for instance, in construction of patient-specific template guides and manufacturing spine replica for preoperative planning and surgical training [7–11]. However, so far there is still no literature about bone surrogates for haptically realistic simulation of spinal surgical procedures.

The purpose of this study was to validate haptics and biomechanics during surgical simulation of pedicle screw insertion and decompression surgery using a parameterizable vertebra model that is configurable in cortical and cancellous bone properties. We hypothesized that adjusting parameters of this model can lead to bone density-specific vertebrae with tactile behavior similar to real vertebrae with normal and osteoporotic bone quality. Further, we aimed to provide an outlook toward the future potential in preoperative haptic simulation of spine surgery on patient-specific spine replicas based on this parameterizable vertebra model.

Materials and methods

Computer-aided modeling

As a template for the outer shape of the 3D-printed vertebrae, a commercially available L3 surgical training vertebra (Model 1378603; Sawbones®, Vashon, WA, USA) (Sawbones) was used. A CT scan of the Sawbones was acquired with a slice thickness of 1 mm. Afterward, segmentation, 3D reconstruction, and transformation to the standard triangulation language (STL) format of the image data were performed with specialized software (MIMICS®, Materialise, Leuven, Belgium). This data format represented the outer shape of the 3D-printed vertebrae and served as a base for the development of a parameterizable model, adjustable in cortical and cancellous bone parts, i.e., general cortical thickness (GCT), lateral pedicle cortical thickness (LPCT), medial pedicle cortical thickness (MPCT), and trabecular thickness (TT). Adjusting these parameters was performed with the 3D modeling software Netfabb (Autodesk®, San Rafael, CA, USA) and CASPA® (Balgrist CARD AG, Zurich, Switzerland).

Cancellous and cortical bones were differentiated by configuring a regular internal offset from the outer shape (GCT), with the envelope functionality of Netfabb (Fig. 1a). Emphasis was placed on realistic proportions in lateral and medial pedicle wall thickness (LPCT and MPCT) as this region is crucial for the training of correct pedicle screw placement. 3D-designed lateral and medial hemicylinders of which the radii were defined as pedicle radius minus desired LPCT and MPCT, respectively, were placed in the pedicle centrally (Fig. 1a, b). Subtracting the hemicylinders from the cortex led to the desired pedicle cortex diameters. Finally, to allow

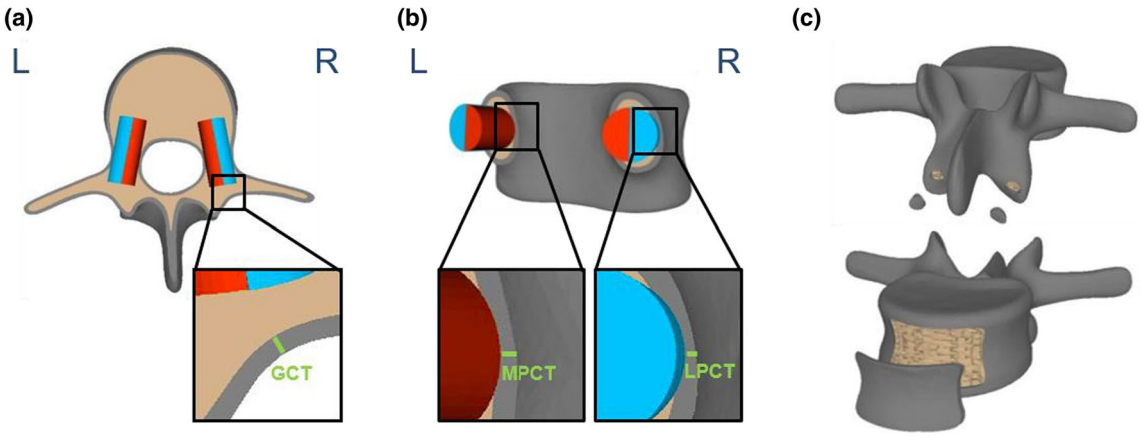

Fig. 1 Illustration of processes during 3D modeling. **a** View from superior on vertebra cut in a transversal plane at pedicle level. Gray: outer part (cortex). Brown: inner part (cancellous). Red: medial hemicylinder. Blue: lateral hemicylinder; GCT, general cortical thickness. **b** View from posterolateral on vertebra cut in the coronal plane at pedicle level. MPCT, medial pedicle cortical thickness; LPCT, lateral pedicle cortical thickness. **c** Cortex openings and covers for removal of support material after 3D printing

the removal of the support material after 3D printing, openings and covers in the cortical structures were 3D-designed at points uninvolved in the following surgical simulation, namely at the inferior articular process and ventral vertebral body (Fig. 1c).

The gyroid, a mathematical minimal surface structure, was used for simplification and parameterization of cancellous bone (Fig. 2a). The mathematical gyroid equation $0 = \sin(c*x)*\cos(c*y)+\sin(c*y)*\cos(c*z)+\sin(c*z)*\cos(c*x)$, was transformed to a 3D surface model with Netfabb, where c is a constant to control scaling of the structure. In all vertebrae, we used $c = 2.5$, leading to a 250% scaling of proportions. A block of gyroid was 3D-constructed in the size of the inner part of the vertebra with an accuracy of the 3D surface of 0.7 mm. The shape of the cancellous bone of the vertebra was achieved by intersecting the inner part of the vertebra and the gyroid block (Fig. 2b).

An initial vertebra α was designed that took into account findings of anatomic studies on L3 vertebrae [12, 13], by accordingly adjusting the configurable parameters GCT, LPCT, MPCT, and TT (Table 1). LPCT in vertebra α was set to 0.6 mm and MPCT to 0.8 mm, which was in an LPCT/MPCT ratio of 3:4, and the trabecular thickness was set to 0.2 mm. Four additional vertebrae were 3D-designed using the same method, in which values for cortical and trabecular thickness were decreased (β) and gradually increased (γ1, γ2, and γ3), respectively. The LPCT/MPCT ratio of 3:4 was kept in all vertebrae. In relation to vertebra α, LPCT and MPCT were decreased to 50% in β and increased to 200% in γ1, 300% in γ2, and 400% in γ3.

Table 1 Parameters configured in 3D-printed vertebrae

Vertebra	GCT (mm)	LPCT (mm)	MPCT (mm)	TT (mm)
α	1.3	0.6	0.8	0.2
β	1.1	0.3	0.4	0.15
γ1	1.7	1.2	1.6	0.3
γ2	2.6	1.8	2.4	0.4
γ3	3.4	2.4	3.2	0.5

GCT general cortical thickness, *LPCT* lateral pedicle cortical thickness, *MPCT* medial pedicle cortical thickness, *TT* trabecular thickness

3D printing

Rapid prototyping multijet printing technology (Projet MJP 5500 X, 3D Systems, Rock Hill, SC, USA) was used with a print accuracy of 16 µm. Vertebrae were printed with composites of hard rigid materials of translucent clear color (VisiJet® CR-CL 200, 3D Systems, Rock Hill, SC, USA) (CR-CL) and soft elastomeric material of black color (VisiJet® CE-BK, 3D Systems, Rock Hill, SC, USA) (CE-BK). Mixing proportions of the vertebra cortex were set to 75% CR-CL and 25% CE-BK (CL-BK-75) and for the cancellous bone to 100% CR-CL. 3D-printed material properties are presented in Table 2. During print processes, the printer uses an additional material (VisiJet® S500, 3D Systems, Rock Hill, SC, USA) (S500) to support freestanding features and to fill voids inside the cancellous bone meshwork. Removal of S500 through the dedicated ventral and dorsal cortical holes was then performed at 62 °C in a convection oven and under mechanical centrifugation. Subsequently, the vertebrae underwent cleaning in the ultrasonic bath (Elma Elmasonic S 450 H, Singen, Germany) at 62 °C filled with cleaning liquid Dewax RP/5 (Steiner Werkzeugmaschinen AG, Gränichen, Switzerland). After a water bath and drying overnight, the cortex openings were sealed with the corresponding covers and a tip of superglue. All vertebrae were finally colored white with an acryl spray to eliminate color differences.

Surgical evaluation

Four test setups were prepared, each consisting of five 3D-printed vertebrae α, β, γ1, γ2, γ3, and one Sawbones, all randomly arranged (Fig. 3a). The vertebra models were positioned in a dedicated frame without rigid fixation. An

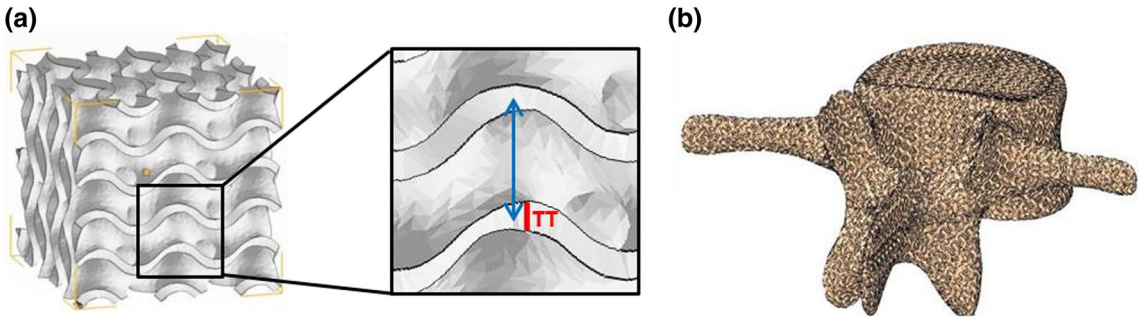

Fig. 2 **a** Gyroid structure for simulation of cancellous bone. TS, trabecular spacing; TT, trabecular thickness. **b** Intersection between gyroid block and inner part of the vertebra

Table 2 3D-printed material properties

Properties	CR-CL	CE-BK	CL-BK-75
Use in this study	Cortical bone	N/A	Cancellous bone
Composition	UV curable plastic	UV curable elastomeric	75% CR-CL, 25% CE-BK
Description	Rigid, polycarbonate-like	Elastomeric	Semirigid
Color	Translucent clear	Opaque black	Semitranslucent gray
Tensile strength (N/mm^2)	37–47	0.2–0.4	19–27
Flexural strength (N/mm^2)	61–72	N/A	18–21
Flexural modulus (N/mm^2)	1400–2000	N/A	450–750
Impact strength (kJ/m^2)	16–19	N/A	18–25
Shore A hardness	N/A	27–33	N/A
Shore D hardness	76–80	N/A	70–80
Tear resistance (N/mm)	N/A	3.1–3.7	N/A

CR-CL = VisiJet® CR-CL 200; CE-BK = VisiJet® CE-BK; CL-BK-75 = mixture of 75% CR-CL and 25% CE-BK; exact material compositions are kept secret by 3D Systems

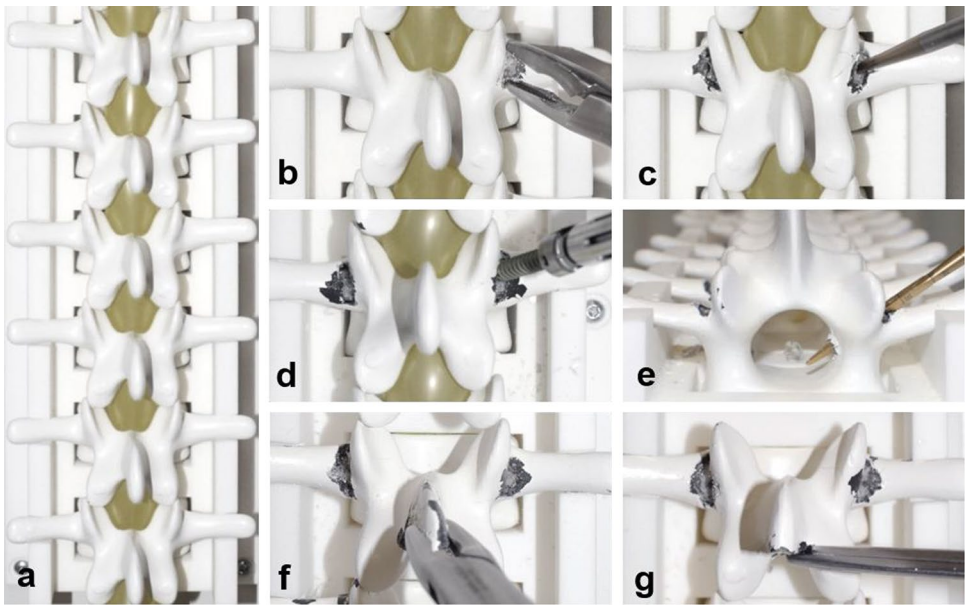

Fig. 3 Steps during surgical evaluation. **a** Test setup of six different vertebrae. **b** Step 1: Bilateral opening of the cortex at the pedicle screw insertion sites. **c** Step 2: Pilot hole preparation. **d** Step 3: Insertion of a polyaxial pedicle screw. **e** Step 4: Pilot hole preparation on the opposite side in inappropriate trajectory with intentional perforation of the medial pedicle cortex. **f** Step 5: Removal of the spinous process. **g** Step 6: Laminotomy

air-filled balloon was used to simulate the spinal cord. Three orthopedic surgeons and one neurosurgeon, all board-certified and spine surgery trained, each assessed a test setup. Six common surgical steps in posterior spondylodesis surgery were evaluated. In the first step, the surgeons opened the cortex at the pedicle screw insertion sites with a Luer rongeur bilaterally (Fig. 3b). The second step was preparing a pilot hole with a 3.2-mm Lenke probe (Expedium, DePuy Synthes, PA, USA) in appropriate trajectory on one side (Fig. 3c). In step three, a 6.0 mm × 45 mm polyaxial pedicle screw (SI, Expedium, DePuy Synthes) was inserted with freehand technique (Fig. 3d). During step four, the surgeons had to deliberately perform an inappropriate pilot hole preparation and intentional violation of the lateral and medial pedicle wall with the Lenke probe (Fig. 3e). Step five was removal of the spinous process with Luer rongeurs (Fig. 3f). The last step was laminotomy with Kerrison rongeurs (Fig. 3g). Each surgeon subjectively assessed haptic behavior during all surgical evaluation steps with a scale comprising increasing levels of hardness: 1–2 too soft for real bone, 3–4 osteoporotic-like bone quality, 5–6 normal bone quality, 7–8 hard bone quality, and 9–10 too hard for a realistic bone (Fig. 4). All surgeons evaluated the vertebrae independently without knowing each other's ratings. Finally, all surgeons conducted a final global assessment about which of the vertebrae was the most realistic for a normal and which for an osteoporotic vertebra.

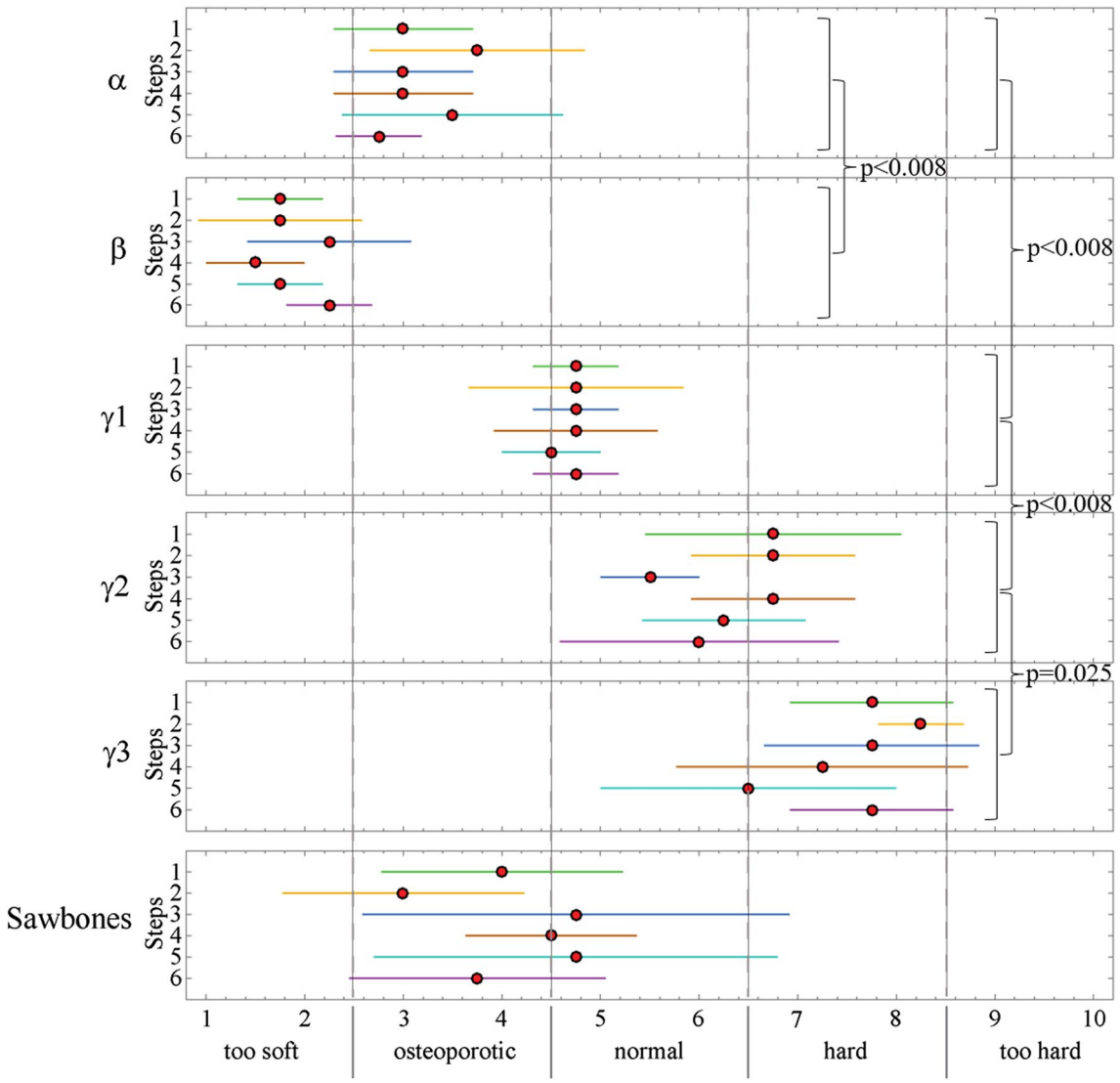

Fig. 4 Scores of each step in surgical evaluation of vertebrae surrogates. Red dot: mean. Whisker: standard deviation. Statistical significance with $p < 0.008$ was found between all vertebrae types, except γ2 and γ3 ($p = 0.025$), and between Sawbones and α ($p = 0.150$) and Sawbones and γ1 ($p = 1.000$)

Torque measurement

During the surgical evaluation, pedicle insertion torques (49 readings per second) were measured with a handy digital torque gauge attached to the screwdriver (Mark-10 M3i Series, New York, NY, USA). Maximum insertion torque and time course of torque of each pedicle screw were registered and compared to studies with similar torque measurement methods and screws (diameters 6.0–6.5 mm) [14–16].

Statistics

Statistical analysis was performed using R version 3.3.3 (R Core Team, Vienna, Austria). Scores of all surgical evaluation steps of a vertebra were pooled, and pairwise Wilcoxon tests were performed. A Bonferroni correction was applied and statistical significance was set at $p < 0.008$ $\left(= \frac{0.05}{6}\right)$. To verify the degree of the inter-rater agreement, Kendall's coefficient of concordance was assessed.

Results

Surgical evaluation of L3 vertebrae

In total, 24 synthetic vertebrae, six vertebrae per each of the four spine surgeons, were evaluated. Inter-rater agreement

was strong with a Kendall's W coefficient of 0.822. Steps one to six were rated with similar scores within types of vertebrae (Fig. 4). Average surgical score in vertebra α was 3.2 ± 0.9 (osteoporotic), β 1.9 ± 0.7 (too soft), γ1 4.7 ± 0.9 (osteoporotic–normal), γ2 6.3 ± 1.1 (normal–hard), and γ3 7.5 ± 1.1 (hard). Statistically significant differences ($p < 0.008$) were found between all 3D-printed vertebra types, except γ2 and γ3 ($p = 0.025$). Mean score of Sawbones was 4.1 ± 1.7 (osteoporotic–normal), and no significant difference was found between Sawbones and α ($p = 0.150$) and Sawbones and γ1 ($p = 1.000$).

All surgeons considered the 3D-printed vertebrae α, γ1, and γ2 as more authentic in haptic behavior than Sawbones. Two surgeons rated vertebrae γ1 as best for the simulation of normal bone properties and α as best for osteoporotic bone, whereas the other two surgeons considered γ2 as most suitable for normal bone and γ1 for osteoporotic bone. Sawbones was criticized for a brittle cortical and rubber-like cancellous bone structure by all surgeons in comparison with the 3D-printed vertebrae which was why the 3D-printed vertebrae were considered superior. Besides the haptic feel, surgeons appreciated authentic acoustic feedback during pilot hole preparation and pedicle screw insertion in the 3D-printed vertebrae.

Pedicle screw insertion torques

Peak torques during pedicle screw insertion were 32 ± 4 Ncm in vertebra α, 12 ± 3 Ncm in β, 74 ± 4 Ncm in γ1, 129 ± 13 Ncm in γ2, 196 ± 34 Ncm in γ3, and 90 ± 11 Ncm in Sawbones (Table 3). After reviewing the literature, we found that average torques of pedicle screws with similar diameters (6.0–6.5 mm) in non-osteoporotic vertebrae ranged from 63 to 129 Ncm (Table 3) [14–16]. Vertebrae γ1, γ2, and Sawbones were within, α and β were below, and γ3 was above this range. These results confirm the subjective surgical scores of step 3 (pedicle screw insertion) which were on average in the normal bone range in γ1, γ2, and Sawbones (Fig. 4). Time courses of torques during screw insertion displayed realistic profiles in vertebrae α, γ1, γ2, γ3, and Sawbones and could be allocated to type B torque patterns according to Bühler et al. [14] (Fig. 5).

Discussion

Posterior spinal fusion surgery belongs in experienced hands, but until today no consensus has been reached on the optimal education of these procedures. Cadaver spines offer the possibility to practice in a low-stress environment [3, 17]. However, cadaver preparation is elaborate and expensive, access may be limited, and cadaver spines do

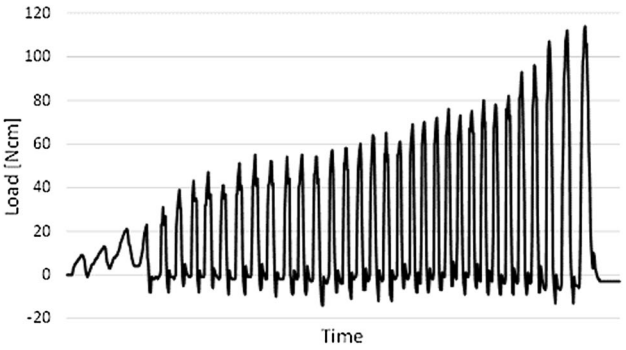

Fig. 5 Example of a pedicle screw insertion torque profile of vertebra γ2. Torque peaks increase after each screw drill, which is in concordance with torque pattern type B according to Bühler et al. [14]

Table 3 Pedicle screw insertion torques: a review of studies in comparison with the present study

Study	Specimen	Screw type	Screw size (mm)	No. of screws	Mean peak torque ± SD (Ncm)
Present study	L3 surrogate, α	Synthes Expedium	6.0 × 45	4	32 ± 4
	L3 surrogate, β	Synthes Expedium	6.0 × 45	4	12 ± 3
	L3 surrogate, γ1	Synthes Expedium	6.0 × 45	4	74 ± 4
	L3 surrogate, γ2	Synthes Expedium	6.0 × 45	4	129 ± 13
	L3 surrogate, γ3	Synthes Expedium	6.0 × 45	4	196 ± 34
	L3 surrogate, Sawbones	Synthes Expedium	6.0 × 45	4	90 ± 11
Bühler et al. [14]	L2-S1, in vivo	Synthes USS	6.0 × 35–45	43	129 ± 56
	L2-S1, in vitro	Synthes USS	6.0 × 35–45	38	67 ± 19
Kwok et al. [15]	L4-L5, in vitro	TSRH	6.5 × 40	11	111 ± 76
	L4-L5, in vitro	Steffee VSP	6.25 × 40	15	63 ± 28
	L4-L5, in vitro	Synthes USS	6.5 × 30	11	117 ± 49
Sandén et al. [16]	L3-S1, in vivo	SAF 2507 Anatomica	6.0 × 55–70	32	76 ± 41

not sufficiently represent the broad spectrum of patient's anatomies and pathologies undergoing spine surgery [6]. To overcome these disadvantages, commercially available surrogate spine models have been introduced for surgical training [18]. Further, computer-assisted and virtual reality-based simulators have been developed for training [19, 20]. The value of these simulation methods remains unclear, and to our knowledge, none of these models provide a satisfactory haptic feel of a human vertebra.

3D printing is a useful tool for manufacturing replica for surgical education with steep learning curves [8–10]. Park et al. first described the usability of patient-specific 3D-printed spine replica for surgical training of pedicle screw fixation with freehand technique and reported a noticeable progression of skills after instrumenting on a few models [8]. However, their study did not focus on haptic authenticity. Further potentials of patient-specific bone replicas have been suggested for improved patient consent and the use for preclinical tests of new surgical techniques [21, 22].

As standard CT scans are not accurate enough to capture the delicate bony architecture of a vertebra in detail, we aimed to create a simplified parameterizable vertebra model that is transferable to a patient's anatomy and bone density. Our goal was to address human anatomic proportions in the design of our vertebra model to gain realistic haptic properties. Inceoglu et al.' anatomic studies on adult L3 cadaveric specimen revealed an average LPCT of 0.6 ± 0.2 mm, MPCT of 0.8 ± 0.2 mm, a TT of 0.2 ± 0.1 mm and spacing between cancellous bone trabeculae of 0.9 ± 0.1 mm, and that trabeculae are of somewhat isotropic plate-like shapes [12, 13]. In line with their results, we initially designed vertebra α by applying the same parameters and by using a cancellous bone structure called gyroid, which roughly fulfills the description of isotropic plate-like trabeculae. By scaling to 250%, spacing between trabeculae of about 0.9 mm was achieved. The gyroid structure has been commonly used in the development of orthopedic implants in recent years, because of its cancellous bone-like mechanical properties [23, 24]. By developing four additional vertebrae (β, γ1, γ2, and γ3), we aimed to print a spectrum from soft to hard vertebrae. In the surgical evaluation, vertebra α was rated as osteoporotic, even though anatomic parameters were set to non-osteoporotic values according to Inceoglu et al. [12, 13]. However, Mughir et al. found thicker pedicle cortices of 1.4 ± 1.6 mm and 1.7 ± 1.2 mm, respectively, which supports that vertebrae γ1 and γ2 best represented normal bone haptics and biomechanics in our study [25].

Our approach offers vertebrae with different bone densities and is further applicable to patient-specific utilization. We herein demonstrate the first step toward preoperative haptic simulation on individual spine replicas (Fig. 6). The outer shape of the showcased replica is based on a patient's spinal CT scan, and the inner form of the vertebrae was artificially modeled using parameters of vertebra γ1. To our knowledge, this is the first patient-specific spine replica with realistic haptic properties for surgical training. Such spine replica could revolutionize preoperative planning by visual and haptic surgical simulation before the real surgery in the future [8, 11].

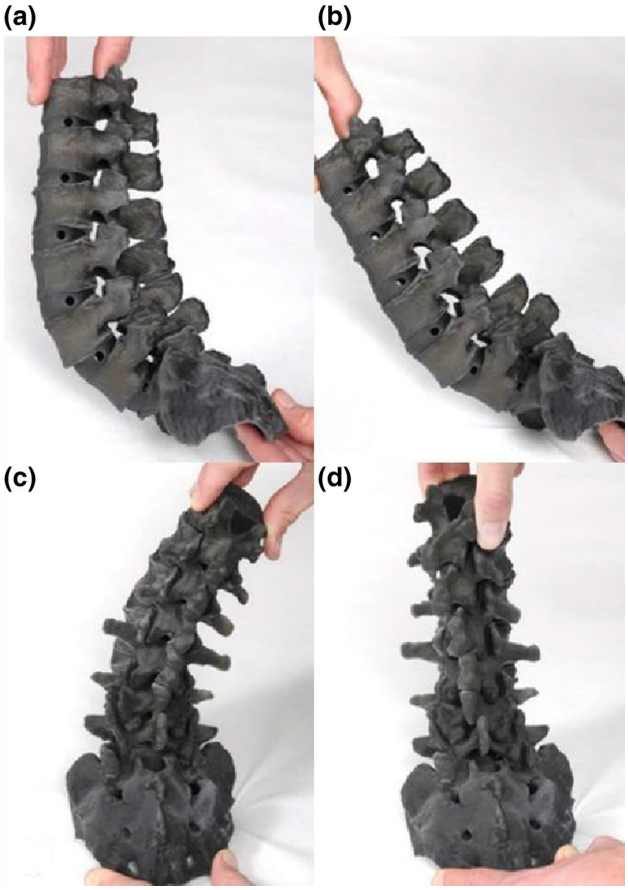

Fig. 6 Showcase of an individual spine surrogate from T12 to sacrum based on a patient's CT scan. Parameters used for vertebra γ1 were set in each vertebra. Elastic intervertebral disks were designed in the form of ellipsoidal rings with lateral holes and 3D-printed with VisiJet® CE-BK. **a** Neutral position. **b** Ventral flexion. **c** Right lateral flexion. **d** Right rotation

Drawbacks of our 3D-printed vertebrae are the material costs of currently around 250 USD per vertebra and the elaborate pre- and post-processing. Further studies should focus on additional biomechanical testings. The usability of patient-specific 3D-printed vertebrae should further be verified in the clinical setting.

Conclusions

The developed parameterizable vertebra model offers realistic vertebrae surrogates regarding haptics and biomechanics during simulation of pedicle screw insertion and posterior

decompression. Bone density-specific vertebrae with normal and osteoporotic haptic properties outperformed conventional Sawbones models in the surgical evaluation. This study further represents the first step toward patient-specific 3D-printed spine replicas, which allow visual and haptic simulation of spine surgery before operating on the real patient.

Acknowledgements The authors are grateful to Dr. Michael Betz, Dr. José Spirig, and Dr. Cyrill Dennler, Department of Spine Surgery, Balgrist University Hospital, for thoroughly assessing the vertebrae surrogates and to Dr. Lazaros Vlachopoulos, Fabio Carrillo, and Michael Hecht, Computer-Assisted Research and Development Group, Balgrist University Hospital, for their helpful support in the vertebrae construction. The authors gratefully acknowledge generous financial support by the Canton of Zurich (HSM II grant).

Compliance with ethical standards

Conflict of interest All authors declare that they have no conflict of interest.

Ethical approval The presented study was conducted in accordance with Swiss and international law requirements. Ethical board's approval was obtained from the Ethical Committee of the Canton of Zurich, Switzerland (ID: BASEC Req-2017-00334).

References

1. Boos N, Webb JK (1997) Pedicle screw fixation in spinal disorders: a European view. Eur Spine J 6:2–18. https://doi.org/10.1007/BF01676569
2. Rajaee SS, Bae HW, Kanim LEA, Delamarter RB (2012) Spinal fusion in the United States: analysis of trends from 1998 to 2008. Spine (Phila Pa 1976) 37:67–76. https://doi.org/10.1097/BRS.0b013e31820cccfb
3. Bergeson RK, Schwend RM, Delucia T et al (2008) How accurately do novice surgeons place thoracic pedicle screws with the free hand technique? Spine (Phila Pa 1976) 33:501–507. https://doi.org/10.1097/BRS.0b013e31817b61af
4. Faraj AA, Webb JK (1997) Early complications of spinal pedicle screw. Eur Spine J 6:324–326. https://doi.org/10.1007/BF01142678
5. Parker SL, Amin AG, Santiago-Dieppa D et al (2014) Incidence and clinical significance of vascular encroachment resulting from freehand placement of pedicle screws in the thoracic and lumbar spine. Spine (Phila Pa 1976) 39:683–687. https://doi.org/10.1097/BRS.0000000000000221
6. Atesok K, Mabrey JD, Jazrawi LM, Egol KA (2012) Surgical simulation in orthopaedic training. J Am Acad Orthop Surg 20:410–422. https://doi.org/10.5435/JAAOS-20-06-410
7. Farshad M, Betz M, Farshad-Amacker NA, Moser M (2017) Accuracy of patient-specific template-guided vs. free-hand fluoroscopically controlled pedicle screw placement in the thoracic and lumbar spine: a randomized cadaveric study. Eur Spine J 26:738–749. https://doi.org/10.1007/s00586-016-4728-5
8. Park HJ, Wang C, Choi KH, Kim HN (2018) Use of a life-size three-dimensional-printed spine model for pedicle screw instrumentation training. J Orthop Surg Res 13:86–95. https://doi.org/10.1186/s13018-018-0788-z
9. Waran V, Narayanan V, Karuppiah R et al (2014) Utility of multimaterial 3D printers in creating models with pathological entities to enhance the training experience of neurosurgeons. J Neurosurg 120:489–492. https://doi.org/10.3171/2013.11.JNS131066
10. Jones DB, Sung R, Weinberg C et al (2016) Three-dimensional modeling may improve surgical education and clinical practice. Surg Innov 23:189–195. https://doi.org/10.1177/1553350615607641
11. Paiva WS, Amorim R, Bezerra DAF, Masini M (2007) Application of the stereolithography technique in complex spine surgery. Arq Neuropsiquiatr 65:443–445. https://doi.org/10.1590/S0004-282X2007000300015
12. Inceoglu S, Burghardt A, Akbay A et al (2005) Trabecular architecture of lumbar vertebral pedicle. Spine (Phila Pa 1976) 30:1485–1490
13. Inceoglu S, Kilincer C, Tami A, Mclain RF (2007) Cortex of the pedicle of the vertebral arch. Part II: microstructure. J Neurosurg Spine 7:347–351. https://doi.org/10.3171/SPI-07/09/347
14. Bühler DW, Berlemann U, Oxland TR, Nolte LP (1998) Moments and forces during pedicle screw insertion. In vitro and in vivo measurements. Spine (Phila Pa 1976) 23:1220–1228
15. Kwok AW, Finkelstein JA, Woodside T et al (1996) Insertional torque and pull-out strengths of conical and cylindrical pedicle screws in cadaveric bone. Spine (Phila Pa 1976) 21:2429–2434
16. Sandén B, Olerud C, Larsson S, Robinson Y (2010) Insertion torque is not a good predictor of pedicle screw loosening after spinal instrumentation: a prospective study in 8 patients. Patient Saf Surg 4:14–18
17. Tomlinson JE, Yiasemidou M, Watts AL et al (2016) Cadaveric spinal surgery simulation: a comparison of cadaver types. Glob Spine J 6:357–361. https://doi.org/10.1055/s-0035-1563724
18. Tanner G, Vojdani S, Komatsu DE, Barsi JM (2017) Development of a saw bones model for training pedicle screw placement in scoliosis. BMC Res Notes 10:678–682. https://doi.org/10.1186/s13104-017-3029-3
19. Ryu WHA, Mostafa AE, Dharampal N et al (2017) Design-based comparison of spine surgery simulators: optimizing educational features of surgical simulators. World Neurosurg 106:870–877. https://doi.org/10.1016/j.wneu.2017.07.021
20. Pfandler M, Lazarovici M, Stefan P et al (2017) Virtual reality-based simulators for spine surgery: a systematic review. Spine J 17:1352–1363. https://doi.org/10.1016/j.spinee.2017.05.016
21. Liew Y, Beveridge E, Demetriades AK, Hughes MA (2015) 3D printing of patient-specific anatomy: a tool to improve patient consent and enhance imaging interpretation by trainees. Br J Neurosurg 29:712–714. https://doi.org/10.3109/02688697.2015.1026799
22. Wu AM, Shao ZX, Wang JS et al (2015) The accuracy of a method for printing three- dimensional spinal models. PLoS ONE 10:1–11. https://doi.org/10.1371/journal.pone.0124291
23. Yánez A, Herrera A, Martel O et al (2016) Compressive behaviour of gyroid lattice structures for human cancellous bone implant applications. Mater Sci Eng C 68:445–448. https://doi.org/10.1016/j.msec.2016.06.016
24. Ali D, Sen S (2017) Finite element analysis of mechanical behavior, permeability and fluid induced wall shear stress of high porosity scaffolds with gyroid and lattice-based architectures. J Mech Behav Biomed Mater 75:262–270. https://doi.org/10.1016/j.jmbbm.2017.07.035
25. Mughir AMA, Yusof MI, Abdullah S, Ahmad S (2010) Morphological comparison between adolescent and adult lumbar pedicles using computerised tomography scanning. Surg Radiol Anat 32:587–592. https://doi.org/10.1007/s00276-009-0612-x

Affiliations

Marco Burkhard[1] · Philipp Fürnstahl[2] · Mazda Farshad[1]

[1] Department of Orthopaedics, Balgrist University Hospital, University of Zurich, Zurich, Switzerland

[2] Computer-Assisted Research and Development Group, Balgrist University Hospital, University of Zurich, Zurich, Switzerland